The Journal of Immunology

Reduced Annexin A1 Expression Associates with Disease Severity and Inflammation in Multiple Sclerosis Patients

Alessandra Colamatteo, Elisa Maggioli, Rodrigo Azevedo Loiola, Madeeha Hamid Sheikh, Gaetano Calì, Dario Bruzzese, Giorgia Teresa Maniscalco, Diego Centonze, Fabio Buttari, Roberta Lanzillo, Francesco Perna, Bruno Zuccarelli, Maria Mottola, Silvana Cassano, Mario Galgani, Egle Solito and Veronica De Rosa

J Immunol 2019; 203:1753-1765; Prepublished online 28 August 2019;
doi: 10.4049/jimmunol.1801683
http://www.jimmunol.org/content/203/7/1753

The Journal of Immunology is published twice each month by
The American Association of Immunologists, Inc.,
1451 Rockville Pike, Suite 650, Rockville, MD 20852

Print ISSN: 0022-1767 Online ISSN: 1550-6606.

Reduced Annexin A1 Expression Associates with Disease Severity and Inflammation in Multiple Sclerosis Patients

Alessandra Colamatteo,* Elisa Maggioli,† Rodrigo Azevedo Loiola,† Madeeha Hamid Sheikh,† Gaetano Calì,‡ Dario Bruzzese,§ Giorgia Teresa Maniscalco,¶ Diego Centonze,‖,# Fabio Buttari,‖ Roberta Lanzillo, Francesco Perna,†† Bruno Zuccarelli,‡‡ Maria Mottola,‡‡ Silvana Cassano,‡ Mario Galgani,‡ Egle Solito,*,†,[1] and Veronica De Rosa‡,§§,[1]**

Chronic neuroinflammation is a key pathological hallmark of multiple sclerosis (MS) that suggests that resolution of inflammation by specialized proresolving molecules is dysregulated in the disease. Annexin A1 (ANXA1) is a protein induced by glucocorticoids that facilitates resolution of inflammation through several mechanisms that include an inhibition of leukocyte recruitment and activation. In this study, we investigated the ability of ANXA1 to influence T cell effector function in relapsing/remitting MS (RRMS), an autoimmune disease sustained by proinflammatory Th1/Th17 cells. Circulating expression levels of ANXA1 in naive-to-treatment RRMS subjects inversely correlated with disease score and progression. At the cellular level, there was an impaired ANXA1 production by $CD4^+CD25^-$ conventional T and $CD4^+ROR\gamma t^+$ T (Th17) cells from RRMS subjects that associated with an increased migratory capacity in an in vitro model of blood brain barrier. Mechanistically, ANXA1 impaired monocyte maturation secondarily to STAT3 hyperactivation and potently reduced T cell activation, proliferation, and glycolysis. Together, these findings identify impaired disease resolution pathways in RRMS caused by dysregulated ANXA1 expression that could represent new potential therapeutic targets in RRMS. *The Journal of Immunology*, **2019, 203: 1753–1765.**

Inflammation is a fundamental host defense process mounted in response to chemical, physical lesions, or microbial infection, which results in edema formation and leukocyte trafficking into the injured site (1). As acute inflammation is accompanied by destruction of the surrounding host tissue, the high-tuned regulation of the duration and severity of the proinflammatory phase is necessary for organ/tissue regain of function (2). However, there are some pathological conditions in which inflammation fails to resolve and persists overtime leading to chronic inflammation, like those occurring in immune-mediated diseases of the CNS, such as multiple sclerosis (MS) (3).

MS is an autoimmune disorder characterized by multifocal areas of demyelination, axonal damage, activation of glial cells, and immune cell infiltration. Although several genetic, environmental, and hormonal factors have been implicated in pathogenesis of MS, the perturbation of endogenous regulatory mechanisms represents an important factor for initiation, maintenance, and lack of resolution of brain inflammation (3). Several cytokines, NO, free radicals, and the abundance of proinflammatory cells such as $CD4^+$ Th1 and Th17 targeting CNS self-antigens have been implicated in MS pathogenesis (4, 5). Despite that many different disease-modifying treatments have become available to reduce frequency of relapses and slow

*Dipartimento di Medicina Molecolare e Biotecnologie Mediche, Università degli Studi di Napoli "Federico II," 80131 Naples, Italy; †William Harvey Research Institute, Barts and The London School of Medicine and Dentistry, Queen Mary University of London, EC1M 6BQ London, United Kingdom; ‡Istituto per l'Endocrinologia e l'Oncologia Sperimentale "G. Salvatore," Consiglio Nazionale delle Ricerche, 80131 Naples, Italy; §Dipartimento di Sanità Pubblica, Università degli Studi di Napoli "Federico II," 80131 Naples, Italy; ¶Dipartimento di Neurologia, Centro Regionale Sclerosi Multipla, Azienda Ospedaliera "A. Cardarelli," 80131 Naples, Italy; ‖Istituto di Ricovero e Cura a Carattere Scientifico Neuromed, 86077 Pozzilli, Italy; #Department of Systems Medicine, Tor Vergata University, 00133 Rome, Italy; **Dipartimento di Neuroscienze e Scienze Riproduttive ed Odontostomatologiche, Università degli Studi di Napoli "Federico II," 80131 Naples, Italy; ††Dipartimento di Medicina Clinica e Chirurgia, Università degli Studi di Napoli "Federico II," 80131 Naples, Italy; ‡‡Unità Operativa Complessa di Medicina Trasfusionale, Azienda Ospedaliera Specialistica dei Colli Monaldi-Cotugno, Centro Traumatologico Ortopedico, 80131 Naples, Italy; and §§Unità di NeuroImmunologia, Fondazione Santa Lucia, 00143 Rome, Italy

[1]E.S. and V.D.R. equally contributed to this work.

ORCIDs: 0000-0003-2901-2374 (G.C.); 0000-0001-9911-4646 (D.B.); 0000-0002-0679-9939 (G.T.M.); 0000-0002-6089-4670 (F.B.); 0000-0003-3817-7920 (M.M.); 0000-0001-9868-7936 (S.C.); 0000-0001-8414-1676 (M.G.); 0000-0001-5279-0049 (E.S.); 0000-0002-9477-0991 (V.D.R.).

Received for publication December 31, 2018. Accepted for publication July 25, 2019.

This work was supported by grants from Fondazione Italiana Sclerosi Multipla (2014/R/21 to V.D.R. and E.S.) and the Ministero della Salute, Bando Ricerca Finalizzata 2016, Giovani Ricercatori (GR-2016-02363725 to V.D.R.). M.G. was supported by grants from the Juvenile Diabetes Research Foundation (JDRF; 2-SRA-2018-479-S-B), the European Foundation for the Study of Diabetes/JDRF/Lilly Programme 2016, and the National Multiple Sclerosis Society (PP-1804-30725).

A.C., R.A.L., E.M., and M.H.S. performed most of the experiments and data analyses; G.C. performed confocal microscopy and data analyses; D.B. and A.C. performed all statistical analyses; M.G. and S.C. were involved in data discussion; G.T.M., D.C., F.B., R.L., F.P., B.Z., and M.M. provided human samples from relapsing/remitting multiple sclerosis or healthy subjects and were involved in data discussion; V.D.R. and E.S. designed the study, analyzed the data, interpreted the results, wrote the manuscript, and supervised the work.

Address correspondence and reprint requests to Dr. Egle Solito or Dr. Veronica De Rosa, Charterhouse Square, EC1M 6BQ London, U.K. (E.S.) or Consiglio Nazionale delle Ricerche, Via Sergio Pansini 5, 80131 Naples, Italy (V.D.R.). E-mail addresses: e.solito@qmul.ac.uk (E.S.) or veronica.derosa@cnr.it (V.D.R.)

The online version of this article contains supplemental material.

Abbreviations used in this article: ANXA1, annexin A1; AS, autologous serum; BBB, blood brain barrier; ECAR, extracellular acidification rate; EDSS, Expanded Disability Status Scale; FPR2, formyl peptide receptor 2; MHC II, MHC class II; MS, multiple sclerosis; r-hANXA1, recombinant human ANXA1; RORγt, RAR-related orphan receptor γ; RRMS, relapsing/remitting MS; Tconv, conventional T; Treg, regulatory T.

disease progression, glucocorticoids are recommended as the standard of care for acute MS flares, thanks to their proven effectiveness to reduce clinical disability and promote the recovery (6, 7). This is also secondary to a direct effect on T cells and blood brain barrier (BBB) during MS (8, 9). Annexin A1 (ANXA1) is considered a primary endogenous mediator of the anti-inflammatory and immunosuppressive actions of glucocorticoids (10). It is expressed abundantly in monocytes and neutrophils, playing an important role in the resolution of inflammation through the control of leukocyte migration, macrophage phagocytosis, and neutrophil apoptosis (11, 12). After cytoplasmic ANXA1 protein is externalized, it interacts with negatively charged phospholipids of membrane and its receptor *N*–formyl peptide receptor 2 (FPR2) (13), activating downstream anti-inflammatory signaling in an autocrine and paracrine manner (inhibition of phospholipase A_2 activity, downregulation of MAPK, and NF-κB activation) (14–16). Despite its well-described inhibitory effect on innate immune responses in vivo and in vitro, its role on adaptive immunity is extremely controversial (17–22). ANXA1 is also expressed in several brain cell types, in particular in microvascular endothelial cells, where it regulates BBB integrity (23). Recently, a selective loss of ANXA1 in the plasma and cerebrovascular endothelium of MS subjects has been reported (23). All these findings pinpoint ANXA1 as a critical component at the interface between the anti-inflammatory regulation of the immune system and the control of the BBB integrity in MS.

In this study, we evaluated how ANXA1 levels correlated with disease clinical score and number of relapses in a cohort of naive-to-treatment relapsing/remitting MS (RRMS) subjects before they underwent standard glucocorticoid administration. This is particularly relevant, as steroids can impact on ANXA1 production, thus affecting our analyses. We also investigated the role of ANXA1 in adaptive immunity by measuring its production in T cell subsets with different roles in MS pathogenesis, including $CD4^+$ conventional T (Tconv) cells, $CD4^+$ Forkhead-box-p3 $(FOXP3)^+$ regulatory T (Treg) cells, and proinflammatory RAR-related orphan receptor γ ($ROR\gamma t^+$) (Th17) cells, also relating the findings to migratory cell capacity in an in vitro BBB model. Finally, we explored whether ANXA1 had a direct anti-inflammatory role on human T cells and whether this process could be altered in MS. We found reduced systemic and T cell–derived expression of ANXA1 that correlated with disease severity in RRMS subjects. At molecular level, ANXA1 affected T cell activation in healthy subjects through a direct interference with T cell priming, and this pathway was hampered in RRMS.

Materials and Methods

Subjects and study design

The study was approved by the Institutional Review Board of the Università degli Studi di Napoli "Federico II" and by the Oxfordshire Research Ethics Committee. RRMS subjects were enrolled by our clinician collaborators at Università degli Studi di Napoli "Federico II," Azienda Ospedaliera di Rilievo Nazionale "Antonio Cardarelli" Napoli, Istituto di Ricovero e Cura a Carattere Scientifico Istituto Neurologico Mediterraneo Neuromed, Pozzilli (Isernia), and Centre for Neuroscience and Trauma, Queen Mary University of London (London, U.K.). Peripheral blood was obtained from RRMS and healthy subjects after they signed a written informed consent approved by institutional review boards. All blood samples were collected at 9:00 AM into heparinized Vacutainers (BD Biosciences) and were processed within the following 4 h. Demographic and clinical characteristics of study cohorts are shown in Table I. All subjects were naive to treatment and with definite RRMS diagnosis, according to the revised McDonald criteria (24). Healthy subjects were matched for age, body mass index, and sex and had no history of inflammation, endocrine, or autoimmune disease, as shown in Table I. The ethnic distribution among the groups was comparable, with all participants being Caucasian.

Cell purification, cultures, and proliferation

PBMCs from healthy and naive-to-treatment RRMS subjects were isolated after Ficoll–Hypaque gradient centrifugation (GE Healthcare). Peripheral $CD4^+$ cells were purified (90–95% pure) from PBMCs of healthy and naive-to-treatment RRMS subjects by magnetic cell separation with Dynabeads Untouched Human CD4 T Cells Kit (Thermo Fisher Scientific). Peripheral Treg ($CD4^+CD25^+CD127^-$) and Tconv ($CD4^+CD25^-$) cells were purified (90–95% pure) from PBMCs of healthy and naive-to-treatment RRMS subjects by magnetic cell separation with a Regulatory $CD4^+CD25^+$ T Cell Kit (Thermo Fisher Scientific). For isolation of monocytes, we stained PBMCs from healthy subjects with APC-conjugated anti-human CD14 (RMO52) (Beckman Coulter) and sorted monocytes by FACSJazz sorter (BD Biosciences) (cell purity > 95%). For proliferation assays, PBMCs were cultured for 60–72 h (1×10^5 cells per well) in flat-bottom, 96-well plates (Corning Falcon) with RPMI 1640 medium supplemented with penicillin (100 UI/ml), streptomycin (100 μg/ml) (Thermo Fisher Scientific), and 5% autologous serum (AS) in the presence or in the absence of anti-CD3 mAb (OKT3) (0.1 μg/ml), treated or not with recombinant human ANXA1 (r-hANXA1) (GTP Technology) (20 μg/ml). Treg and Tconv cells were cultured (1×10^4 cells per well) for 60–72 h in round-bottom, 96-well plates (Corning Falcon) in RPMI 1640 medium supplemented with 5% AS and stimulated with Dynabeads coated with mAb to CD3 plus mAb to CD28 (anti-CD3 + anti-CD28 mAbs) (0.5 beads per cell; Thermo Fisher Scientific), in the presence or in the absence of r-hANXA1 (20 μg/ml). After 60–72 h, [^{3}H]thymidine (0.5 μCi/well; Amersham Pharmacia Biotech) was added to the cell cultures, and cells were harvested 12 h later. Radioactivity was measured with a β cell plate scintillation counter (Wallac). For cytofluorimetric analysis, PBMCs from healthy and naive-to-treatment RRMS subjects were cultured (2×10^6 per well) in flat-bottom, 24-well plates (Corning Falcon) in RPMI 1640 medium supplemented with 5% AS for 12 and 36 h in the presence of anti-CD3 mAb (OKT3) (0.1 μg/ml), treated or not with r-hANXA1 (20 μg/ml). For immunofluorescence and confocal microscopy, $CD4^+$ cells from healthy and naive-to-treatment RRMS subjects were cultured (2×10^6 per well) in flat-bottom, 24-well plates (Corning Falcon) in RPMI 1640 medium supplemented with 5% AS for 12 h, in the presence of anti-CD3 + anti-CD28 mAbs (0.2 bead per cell; Thermo Fisher Scientific). For immunoblot analysis, monocytes were pretreated or not with r-hANXA1 for 1 h (2×10^5 cells per well) in round-bottom, 96-well plates (Corning Falcon), with RPMI 1640 medium supplemented with penicillin (100 UI/ml) and streptomycin (100 μg/ml) (Thermo Fisher Scientific), and then stimulated for 1 h with LPS (1 μg/ml) (Sigma-Aldrich).

ELISA

ANXA1 levels were determined by ELISA (Human Annexin A 1 ELISA Kit [CSB-E12155H]). Briefly, samples were diluted 1:2 and used on a precoated ELISA plate as per manufacturer's instructions. Absorbance was measured using a microplate reader (model 500; Bio-Rad Laboratories, Hercules, CA) and sample readings were extrapolated against a concurrently run standard curve. The values were output as ANXA1 nanograms per milliliter.

Luminex analysis

Fluorescent bead technology was used to assay 50 μl of supernatants from PBMCs culture (24 h) from healthy and naive-to-treatment RRMS subjects. Cytokines levels (IL-1β, IL-10, IL-13, IL-6, IL-12, RANTES, Eotaxin, IL-17A, MIP-1α, GM-CSF, MIP-1β, MCP-1, IL-15, IL-5, IFN-γ, IFN-α, IL-1RA, TNF-α, IL-2, IL-7, IP-10, IL-2R, MIG, IL-4, and IL-8) were measured by using Human Cytokines Magnetic 25-Plex Panel (Novex, Life Technologies). Fluorescence was detected by using Luminex 200 System (Luminex, Austin, TX), and the resulting data were evaluated by using xPONENT Software Version 3.1 (Luminex).

Flow cytometry

Freshly isolated and OKT3-stimulated PBMCs from healthy and naive-to-treatment RRMS subjects were surface stained with the following mAbs: APC-H7–conjugated anti-human CD4 (RPA-T4) and PE-Cy7–conjugated anti-human CD25 (M-A251) (both from BD Biosciences). Thereafter, cells were washed, fixed, and permeabilized (Human FoxP3 Buffer Set; BD Pharmingen) and stained with following mAbs: unconjugated anti-human ANXA1, followed by incubation with secondary Ab Alexa Fluor 488–conjugated anti-rabbit IgG (H chain + L chain) (from Thermo Fisher Scientific), PE-conjugated anti-human FOXP3 (259D/C7), and Alexa Fluor

647–conjugated anti-human RORγt (Q21-559) (all from BD Biosciences). To evaluate ANXA1 surface levels, we stained PBMCs with anti-human ANXA1, followed by incubation with secondary Ab Alexa Fluor 488–conjugated anti-rabbit IgG (H chain + L chain) (from Thermo Fisher Scientific), APC-H7–conjugated anti-human CD4 (RPA-T4), and PE-Cy7–conjugated anti-human CD25 (M-A251) (from BD Biosciences). Thereafter, cells were washed, fixed, and permeabilized (Human FoxP3 Buffer Set; BD Biosciences) and were stained as previously described. For surface staining of PBMCs from healthy and naive-to-treatment RRMS after 36 h of OKT3 stimulation, we used the following mAbs: PE-Cy7–conjugated anti-human CD80 (L307.4), PE-Cy7–conjugated anti-human CD83 (HB15e), PE-conjugated anti-human CD86 (2331) (all from BD Biosciences); FITC-conjugated anti-human CD54 (MCA1615F) (from Bio-Rad Laboratories); and FITC-conjugated anti-human CD19 (J3-119) and PE-conjugated anti-human HLA-DR (Immu-357) (both from Beckman Coulter). For staining of PBMCs from healthy and naive-to-treatment RRMS with anti–human formyl peptide receptor–like 1 (FPRL1) (GM-1D6) from Aldevron, we incubated PBMCs with anti-human FPRL1 in the presence of Fc block (BD Biosciences) for 45 min at 4°C. Then, cells were washed with PBC buffer (PBS plus 0.15% BSA plus 1.32 mM $CaCl_2$) and incubated with secondary Ab, goat anti-mouse Alexa Fluor 488 (from Thermo Fisher Scientific) for 30 min at 4°C diluted 1:300 in PBS. Cells were analyzed with FACSCanto II (BD Biosciences) and FlowJo software (Tree Star). For staining of PBMCs from healthy and naive-to-treatment RRMS subjects after transmigration assay, we fixed cells for 30 min at room temperature with Staining Buffer (PBS plus 2% BSA) containing Alexa Fluor 648–conjugated anti-human CD4 (OKT4) and PE-Cy7–conjugated anti-human CD25 (M-A251), all from BD Biosciences. Then, cells were washed, centrifuged, and collected for the analysis (FACS Fortessa; BD Biosciences), followed by FlowJo software (Tree Star) analysis.

Transmigration assay

As a general model of human in vitro BBB, we used human brain microvascular endothelial cell line (hCMEC/D3), between 26th and 31st passage (25). hCMEC/D3 cells were cultured in tissue culture flasks coated for 2 h at 37°C in rat tail collagen type I solution in EBM-2 medium (Lonza) containing 2.5% (v/v) FBS, as recommended by the manufacturer. Cultures were maintained at 37°C in 5% CO_2, replaced with fresh medium every 3 d, and split when they reached 100% confluence. hCMEC/D3 cells were grown for 72 h on transwell polycarbonate filters (membrane diameter 6.5 mm and 5-μm porosity; Corning) previously coated with calf skin collagen type I (Sigma-Aldrich) and bovine plasma fibronectin (Sigma-Aldrich). EBM-2 medium, containing 5% of AS, was added to the lower compartment of transwell 30 min prior transmigration assay. Then, PBMCs (1×10^6 cells) were suspended in EBM-2 medium containing 5% AS and added to the upper compartment of transwell in contact with hCMEC/D3 monolayer. In some experiments, PBMCs were stimulated for 16 h with anti-CD3 mAb (OKT3) (0.1 μg/ml) and further applied in 5% AS to the endothelial cells for 4 h. The transmigration assays were run during 4 h at 37°C at 5% CO_2. Transmigrated cells were collected from the bottom compartment by aspirating the medium. Cells were fixed with 2% paraformaldehyde for 10 min at room temperature, and staining was performed.

Molecular signaling and immunoblot analysis

Freshly isolated Treg and Tconv cells from naive-to-treatment RRMS and age- and sex-matched healthy subjects were individually stimulated with anti-CD3 + anti-CD28 mAbs (0.1 beads per cell) for 36 h and subsequently pulled before protein extraction. PBMCs from naive-to-treatment RRMS and age- and sex-matched healthy subjects were individually stimulated with OKT3 from 30 min to 12 h, in the presence or in the absence of r-hANXA1 (20 μg/ml), and subsequently pulled before protein extraction. Monocytes were pretreated or not with r-hANXA1 (20 μg/ml) (1 h) and then stimulated for 1 h with LPS (1 μg/ml) (Sigma-Aldrich). Total cell lysates were obtained incubating cells for 20 min at 4°C in Radioimmunoprecipitation assay buffer (R0278; Sigma-Aldrich), plus SIGMAFAST Protease Inhibitor (S8820; Sigma-Aldrich) and Sigma Phosphatase Inhibitor (P5726; Sigma-Aldrich), and immunoblot analyses were performed as described (26). The mAbs used were the following: anti-ANXA1 (1:5000 dilution; Thermo Fisher Scientific), anti–phospho-AKT (Ser473), and AKT (1:1000 dilution; all from Cell Signaling Technology), anti–phospho-ZAP-70 (Tyr49)/Syk (Tyr526) (1:500 dilution; Cell Signaling Technology) and ZAP-70 (1:500 dilution; Santa Cruz Biotechnology), anti–phospho-STAT3 (3E2) and anti-STAT3 (79D7) (1:1000 dilution; all from Cell Signaling Technology), anti–phospho-LCK (Tyr 505) (1:1000 dilution; Cell Signaling Technology), and anti-ERK 1/2 (H-72) (1:1000 dilution; Santa Cruz Biotechnology) to normalize the amount of loaded protein. All filters were quantified by densitometry as described (26). Results were calculated as the densitometry of phosphorylated protein normalized to that of its total form (for AKT, ZAP-70, and STAT3) or normalized to densitometry of ERK 1/2 (for ANXA1 and LCK) and are presented relative to results obtained for either freshly isolated Treg and Tconv cells and 24 h TCR–stimulated Tconv cells from healthy subjects, PBMCs stimulated with OKT3 alone from healthy or naive-to-treatment RRMS subjects, or monocytes treated with LPS alone.

Seahorse metabolic analysis

The metabolic profile was evaluated in PBMCs from healthy and naive-to-treatment RRMS subjects stimulated for 12 h with OKT3 (0.1 μg/ml), in the presence or in the absence of r-hANXA1 (20 μg/ml). Real-time measurements of extracellular acidification rate (ECAR) were made with an XFe96 Extracellular Flux Analyzer (Seahorse Bioscience). PBMCs were plated in XF96 plates (Seahorse Bioscience) at a density of 4×10^5 cells per well and were cultured in RPMI 1640 medium supplemented with 5% AS. ECAR was measured in XF medium in basal conditions and in response to glucose (10 mM), oligomycin (4 μM), and 2-deoxy-D-glucose (2DG) (100 mM) (all from Sigma-Aldrich). Experiments with the Seahorse system were done with the following assay conditions: 3 min of mixture, 3 min of waiting, and 3 min of measurement. Metabolic parameters were then calculated from ECAR profile: basal glycolysis (without addition of any compound), basal glycolysis after glucose injection (after glucose addition), maximal glycolysis (after oligomycin addition), and glycolytic capacity (calculated as the difference between oligomycin-induced ECAR and 2DG-induced ECAR).

Immunofluorescence and confocal microscopy

Confocal microscopy was performed on either freshly isolated or stimulated $CD4^+$ cells with anti-CD3 + anti-CD28 mAbs (0.2 beads per cell; Thermo Fisher Scientific) for 12 h. Fixed cells were treated as described elsewhere (26) and incubated overnight at 4°C with primary Abs: mouse anti-human FOXP3 (236A/E7) from eBioscience and anti-human ANXA1 (71-3400; Thermo Fisher Scientific) diluted 1:100 in PBS. Then cells were washed and incubated for 1 h at room temperature with the secondary Abs: goat anti-mouse Alexa Fluor 488 and goat anti-rabbit Alexa Fluor 594, respectively (from Thermo Fisher Scientific), diluted 1:200 in PBS. For the assessment of ANXA1 surface levels, we stained $CD4^+$ cells with anti-human ANXA1 diluted 1:100 in PBS for 20 min at 4°C, washed and incubated with the secondary Ab goat anti-rabbit Alexa Fluor 594 (from Thermo Fisher Scientific), diluted 1:200 in PBS for 1 h at 4°C. Subsequently, fixed cells were treated as described (26) and incubated overnight at 4°C with primary Ab: mouse anti-human FOXP3 (236A/E7) (from eBioscience), diluted 1:100 in PBS, washed in PBS, and incubated with the secondary Ab, goat anti-mouse Alexa Fluor 488 (from Thermo Fisher Scientific) for 1 h at room temperature diluted 1:200 in PBS. Nuclei were stained with Hoechst. A total of 1.5×10^4 cells were seeded on multitest slide (MP Biomedicals). Immunofluorescence analyses were carried out on an inverted and motorized microscope (Axio Observer Z.1) equipped with a 63×/1.4 Plan-Apochromat Objective. The attached laser-scanning unit (LSM 700 4× pigtailed laser 405-488-555-639; Zeiss, Jena, Germany) enabled confocal imaging. For excitation, 405-, 488-, and 555-nm lasers were used. Fluorescence emission was revealed by Main Dichroic Beam Splitter and Variable Secondary Dichroic Beam Splitter. Triple staining fluorescence images were acquired separately using ZEN 2012 software in the blue, green, and red channels at a resolution of 1024×1024 pixels, with the confocal pinhole set to 1 Airy unit and then saved as TIFF files.

Statistical analysis

Statistical analyses were performed using GraphPad program (Abacus Concepts). Results were expressed as mean ± SEM or SD; a p value ≤ 0.05 was indicative of statistical significance. The nonparametric Wilcoxon matched-pairs signed-rank test and the Mann–Whitney U test were used. We used two-tailed tests for all analyses. To evaluate the relationship between the dependent variables (Expanded Disability Status Scale [EDSS] score and number of relapses prediagnosis) and ANXA1 levels, we computed the nonparametric Spearman rank correlation.

Results

Circulating ANXA1 levels inversely correlate with disease clinical score in naive-to-treatment RRMS subjects

We measured ANXA1 plasma levels in $n = 71$ naive-to-treatment RRMS patients at diagnosis (Table I) to assess whether and how

Table I. Characteristics of naive-to-treatment RRMS (n = 122) and healthy (n = 80) subjects

	RRMS Subjects (n = 122)	Healthy Subjects (n = 80)
Male, n (%)	46 (37.7)	30 (37.5)
Female, n (%)	76 (62.3)	50 (62.5)
Age, mean ± SD, y	36.4 ± 11.1	36.9 ± 11.0
BMI, mean ± SD, kg/m^2	26.3 ± 5.5	24.8 ± 3.1
EDSS at baseline, median [min; max]	2.0 [0.0; 5.0]	—
Disease duration, mean ± SD, y	2.4 ± 4.2	—

BMI, body mass index; max, maximum; min, minimum.

this molecule correlated with the clinical disease status. We evaluated two clinical parameters reflecting disease severity and activity: the Kurtzke EDSS score at baseline and the total number of relapses prediagnosis. Circulating ANXA1 plasma levels ranged from 0.252 to 11.45 ng/ml (median = 1.8; mean ± SD = 2.3 ± 1.9). Its levels were higher in subjects with a lower clinical score (EDSS score < 2) and decreased progressively in those with a higher score (EDSS > 3), reflecting a stronger disability in RRMS. We confirmed the inverse correlation between EDSS score and ANXA1 plasma levels by using the nonparametric Spearman rank correlation (R = 0.239, p = 0.039) (Fig. 1A). To further consolidate this finding, we evaluated the distribution of ANXA1 plasma levels in the same cohort of RRMS subjects stratified into three groups according to the number of relapses prediagnosis. We found that ANXA1 inversely correlated with the number of relapses prediagnosis, as patients with lower levels showed higher number of relapses (Fig. 1B). Taken together, these results suggest that a systemic reduction of ANXA1 secretion could be part of the inflammatory state of RRMS subjects.

Reduced ANXA1 expression in human T cell subsets isolated from naive-to-treatment RRMS subjects

It has been previously reported that innate immune cells, such as neutrophils and monocytes, release ANXA1 (27, 28); however, only few controversial data have been reported on T cells (17–22). To assess whether T cell–derived ANXA1 could be involved in the regulation of adaptive immunity, we evaluated its expression in different CD4$^+$ T cell subsets of healthy individuals, in comparison with naive-to-treatment RRMS patients at diagnosis. We performed a double immunostaining which allowed to measure in parallel total (intracellular plus cell surface) or cell surface ANXA1 levels (29) in two different CD4$^+$ T cell populations, distinct on the basis of their CD25 expression. Cumulative data of the flow cytometric analysis of freshly isolated PBMCs showed that CD4$^+$CD25$^+$ and CD4$^+$CD25$^-$ Tconv cells were enriched for total ANXA1, whereas they expressed low cell surface levels both in healthy and RRMS subjects; also, we observed that total ANXA1 levels were higher in Tconv cells, whereas its cell surface expression was higher in the CD4$^+$CD25$^+$ T cell subset (Fig. 2A, 2B, 2E, 2F, Supplemental Fig. 1A). Interestingly, both total and cell surface ANXA1 levels were significantly reduced in RRMS subjects when compared with healthy donors (Fig. 2A, 2B, 2E, 2F, Supplemental Fig. 1A) being the impairment more significant in the CD4$^+$CD25$^+$ T cell compartment (Fig. 2A, 2E, Supplemental Fig. 1A). Because the CD4$^+$CD25$^+$ T cell subset could represent a mixed cell population, we further analyzed ANXA1 expression by dissecting its levels in two divergent subsets specifically involved in the pathogenesis of MS, namely CD4$^+$FOXP3$^+$ Treg cells and proinflammatory T CD4$^+$RORγt$^+$ (Th17) cells (30, 31). Intriguingly, we observed that, among all the freshly isolated T cell subsets analyzed, the highest expression of ANXA1 was observed in the Th17 compartment, but this was significantly impaired in RRMS (Fig. 2C, Supplemental Fig. 1B). When we measured ANXA1 expression on cell surface, we observed that it was significantly higher in Th17 cells of healthy individuals as compared with RRMS subjects (Fig. 2G, Supplemental Fig. 1B). Analysis of Treg cells showed that total ANXA1 levels were higher in CD4$^+$FOXP3$^-$ cells, whereas its cell surface expression was higher in Treg cells (Fig. 2D, 2H, Supplemental Fig. 1C). Furthermore, ANXA1 expression was significantly reduced in both cellular compartments in RRMS subjects when compared with healthy donors (Fig. 2D, 2H, Supplemental Fig. 1C). These data were also confirmed by Western blot analysis performed in freshly isolated Treg (CD4$^+$CD25$^+$CD127$^-$) and Tconv (CD4$^+$CD25$^-$) cells from RRMS subjects and healthy controls (Supplemental Fig. 2A, 2B). Confocal microscopy of CD4$^+$ T cells freshly isolated from PBMCs of RRMS and healthy subjects, stained for ANXA1 and FOXP3 also confirmed that the expression of ANXA1 was reduced both in CD4$^+$FOXP3$^-$ and Treg cells during MS (Supplemental Fig. 1D). Taken together, our results suggest that a reduction of T cell–derived ANXA1 could be part of the proinflammatory phenomenon observed in MS.

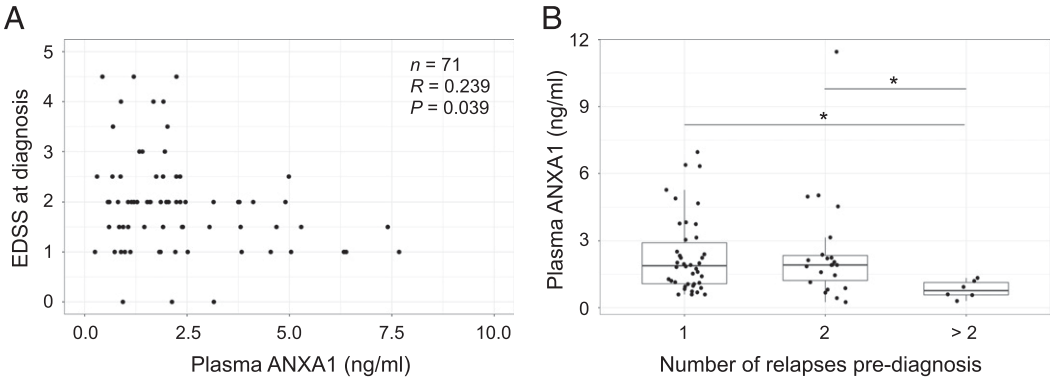

FIGURE 1. ANXA1 levels inversely correlate with clinical status of naive-to-treatment RRMS subjects. (**A**) Correlation between ANXA1 plasma levels and the EDSS score evaluated at diagnosis in naive-to-treatment RRMS subjects (n = 71); correlation has been computed using the nonparametric Spearman rank correlation; R = 0.239, p = 0.039. (**B**) Distribution of ANXA1 plasma levels in naive-to-treatment RRMS subjects (n = 71) stratified into three groups, based on the number of relapses prediagnosis; omnibus test was based on the Kruskal–Wallis nonparametric test, whereas post hoc comparisons were based on the Mann–Whitney U test. *$p \leq 0.05$.

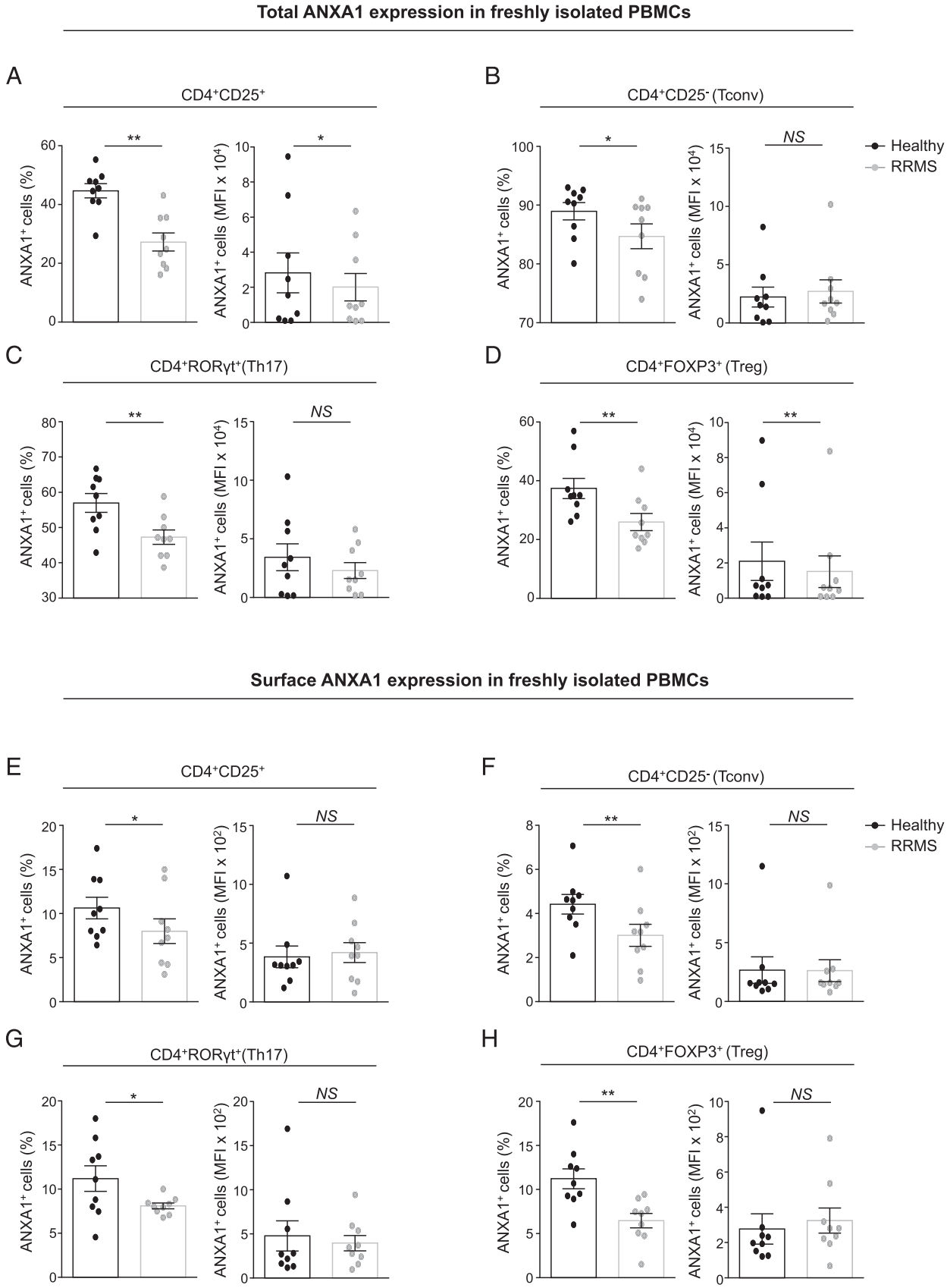

FIGURE 2. ANXA1 expression is reduced in different freshly isolated T cell subsets from naive-to-treatment RRMS as compared with healthy subjects. Histograms show (**A**–**D**) total and (**E**–**H**) surface ANXA1 expression, both as percentages and mean fluorescence intensities (MFI) (referred to the whole population) in (A and E) $CD4^+CD25^+$, (B and F) $CD4^+CD25^-$ (Tconv), (C and G) $CD4^+ROR\gamma t^+$ (Th17), and (D and H) $CD4^+FOXP3^+$ (Treg) cells in freshly isolated PBMCs from healthy ($n = 9$) and naive-to-treatment RRMS ($n = 9$) subjects. Each symbol represents an individual data point. Data are from nine independent experiments; statistical analysis was performed by using paired Wilcoxon test (two tails) (mean ± SEM). $^*p \leq 0.05$, $^{**}p \leq 0.005$.

ANXA1 expression levels are reduced in TCR-stimulated CD4$^+$CD25$^+$, Th17, and Treg cells from naive-to-treatment RRMS subjects

Evidence for physiological function of ANXA1 in modulating inflammation emerged from studies involving ANXA1-null mice and ANXA1 neutralization strategies (19, 22, 32–34). Because the production of anti-inflammatory mediators during the early phases of TCR engagement has a crucial role in T cell fate decision (35), we measured ANXA1 production in CD4$^+$CD25$^+$, Th17, and Treg cells, to evaluate whether an impairment of the endogenous production could occur at this stage in RRMS. Briefly, freshly isolated PBMCs from healthy and RRMS subjects were activated in vitro with mAb anti-CD3 (OKT3, 0.1 μg/ml) and cultured in the presence of 5% AS to preserve their physiological milieu. Twelve hours after activation, CD4$^+$ T cells were analyzed through flow cytometry gating strategy on the basis of their cell surface CD25 expression (reflecting the activation grade) as CD25-high (CD25^{High}), CD25-intermediate (CD25^{Int}) and CD25-low cells to evaluate how the activation status correlated with ANXA1 expression in health and in autoimmunity (Supplemental Fig. 3A). Cumulative data show that, in healthy conditions, the CD4$^+$ T cell subset expressing highest levels of CD25 had strongest expression of ANXA1 (both as cell surface and total levels) (Fig. 3A, 3D, Supplemental Fig. 3A); the same was not true for RRMS subjects, as the CD25^{High} subset expressed significantly lower ANXA1 levels that were comparable to the CD25^{Int} subset (Fig. 3A, 3D, Supplemental Fig. 3A upper and middle panels). Moreover, after TCR engagement, the expression of ANXA1 in the two subsets representing the recently activated T cell pool (CD25^{High} and CD25^{Int}) was impaired in RRMS subjects as compared with healthy individuals (Fig. 3A, 3D, Supplemental Fig. 3A upper and middle panels). We also evaluated whether this could correspond to a different overall activation, evaluated as CD25 expression levels, but we did not observe significant differences in terms of CD25 expression in RRMS compared with healthy subjects (data not shown). Western blot analysis performed with Tconv cells stimulated with anti-CD3/CD28–coated beads for 24 and 36 h also confirmed a substantial reduction in the expression of ANXA1 in RRMS subjects (Supplemental Fig. 2C). All together our data confirmed an impaired T cell–derived ANXA1 production before and after TCR engagement during MS. We next asked whether a defect in ANXA1 production could occur in Th17 cells of RRMS subjects. TCR-stimulated PBMCs (12 h) showed significant impairment of ANXA1 expression in Th17 cells from RRMS subjects when compared with healthy individuals (Fig. 3B, 3E, Supplemental Fig. 3B). FACS analyses of the Treg cell compartment further confirmed the data obtained in freshly isolated Treg cells; indeed, we observed that total ANXA1 levels were higher in CD4$^+$FOXP3$^-$ cells, whereas its cell surface expression was higher in Treg cells (Supplemental Fig. 3C). Moreover, ANXA1 expression was significantly reduced in Treg cells of RRMS subjects when compared with healthy donors (Fig. 3C, 3F, Supplemental Fig. 3C). Confocal microscopy of TCR-stimulated CD4$^+$ T cells stained for ANXA1 and FOXP3 also confirmed that the expression of ANXA1 was reduced in TCR-stimulated CD4$^+$FOXP3$^-$ and Treg cells of RRMS subjects (Supplemental Fig. 3D). Overall, these data suggest a profound impairment of ANXA1 production in RRMS.

Altered migration of T cells from RRMS subjects in an in vitro BBB model

Leukocytes infiltration into the brain is a hallmark of MS disease and several reports suggest a key role for ANXA1 in the regulation of immune cell migration (12, 36). We investigated the behavior of CD4$^+$CD25$^-$ (Tconv), CD4$^+$CD25$^+$, Th17, and Treg cells in contact with polarized human brain microvascular endothelial cell line (hCMEC/D3), an in vitro model of BBB (25). Freshly isolated PBMCs from healthy or naive-to-treatment RRMS subjects were put in contact with hCMEC/D3 cells for 4 h in 5% AS. We observed a significant increase of Tconv cell migration on the endothelium in RRMS as compared with healthy subjects (Fig. 4A). Noteworthy, we did not find a significant difference in CD4$^+$CD25$^+$ T cell migration (data not shown). The same trend was also maintained after 16 h of TCR stimulation (Supplemental Fig. 4A, 4B). Because Th17 cell migration into the CNS represent a major event in MS pathogenesis (37), we better explored this process and found increased migration of Th17 and reduced migration of Treg cells from RRMS subjects across the in vitro model of BBB (Fig. 4B, 4C). These findings suggest that impaired ANXA1 expression levels correlated with increased Tconv and Th17 cell migration in RRMS.

ANXA1 restrains TCR-induced engagement of glycolysis and proliferation in T cells from healthy subjects

We next addressed whether ANXA1 could affect T cell function and activation. To this purpose, we performed a proliferation assay of human PBMCs stimulated with OKT3 in the presence or in the absence of r-hANXA1 (20 μg) in culture medium supplemented with 5% AS to better preserve the in vivo conditions. We observed that addition of exogenous r-hANXA1 to the culture significantly reduced the proliferation of TCR-engaged PBMCs in healthy subjects (~50% of inhibition), whereas the reduction was not statistically significant in naive-to-treatment RRMS individuals (Fig. 5A). Because it is well known that T cells activate a glycolytic program to sustain their own proliferation (38), we evaluated the ECAR, reflecting the glycolytic activity of PBMCs isolated from healthy and naive-to-treatment RRMS subjects upon TCR stimulation (OKT3) in the same culture conditions (5% AS). First, we confirmed that naive-to-treatment RRMS patients had a lower glycolytic engagement compared with healthy controls (39), as testified by reduced glycolytic activity (Fig. 5B, 5C gray versus black lines and columns). Moreover, we found that ANXA1 addition affected glycolysis in TCR-stimulated PBMCs of healthy subjects, whereas it had no effect in RRMS subjects (Fig. 5B, 5C red versus black and blue versus gray lines and columns, respectively). We dissected this molecularly. We performed a time course stimulation (from 30 min to 12 h) for the kinetics of the main pathways related to TCR activation and cytokine/growth-factor signaling and inflammation. We found that r-hANXA1 treatment differently impacted on TCR activation in healthy (n = 6) versus RRMS (n = 6) subjects (Supplemental Fig. 4C, 4D). Indeed, after 30 min of OKT3 stimulation, r-hANXA1 reduced the activation of AKT in PBMCs from healthy, but not RRMS, subjects, where an increased induction was detected (Supplemental Fig. 4C). We also dissected the early events occurring during TCR-activation signaling and found that 2 h treatment with r-hANXA1 of PBMCs from healthy subjects corresponded to a reduction of ZAP-70 activity secondarily to a higher degree of phosphorylation of an inhibitory tyrosine of LCK (Tyr505). In contrast, r-hANXA1 treatment in PBMCs from RRMS subjects led to the induction of ZAP-70 activation because of the lack of LCK phosphorylation (Supplemental Fig. 4D). These results were also paralleled by a slight reduction in the secretion of proinflammatory cytokines (GM-CSF, IL-17A, IFN-α, IL-1RA, IP-10, MCP-1, RANTES, and TNF-α) in PBMCs of healthy individuals, but not in RRMS subjects (data not shown). We asked whether ANXA1 could directly affect the

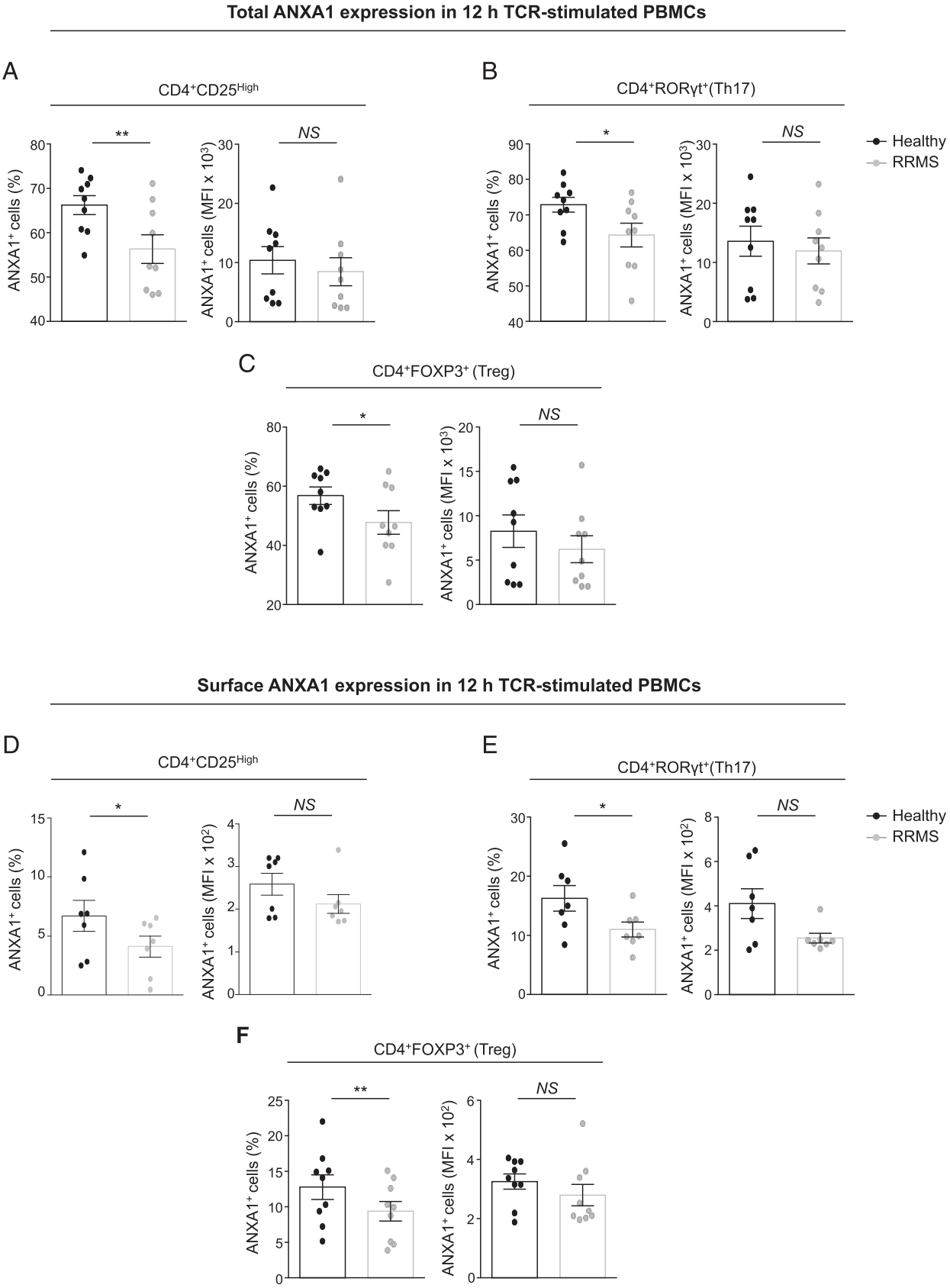

FIGURE 3. ANXA1 expression is reduced in different TCR-stimulated T cell subsets from naive-to-treatment RRMS as compared with healthy subjects. Histograms show (**A**–**C**) total and (**D**–**F**) surface ANXA1 expression, both as percentages and mean fluorescence intensities (MFI) (referred to the whole population) in (A and D) $CD4^+CD25^{High}$, (B and E) $CD4^+ROR\gamma t^+$ (Th17), and (C and F) $CD4^+FOXP3^+$ (Treg) cells in PBMCs from healthy ($n = 9$) and naive-to-treatment RRMS ($n = 9$) subjects after 12 h culture in the presence of TCR stimulation with OKT3. Each symbol represents an individual data point. Data are from seven (surface ANXA1 levels in $CD4^+CD25^{High}$ and $CD4^+ROR\gamma t^+$ [Th17] cells) or nine (all other populations) independent experiments; statistical analysis was performed by using paired Wilcoxon test (two tails) (mean ± SEM). $*p \leq 0.05$, $**p \leq 0.005$.

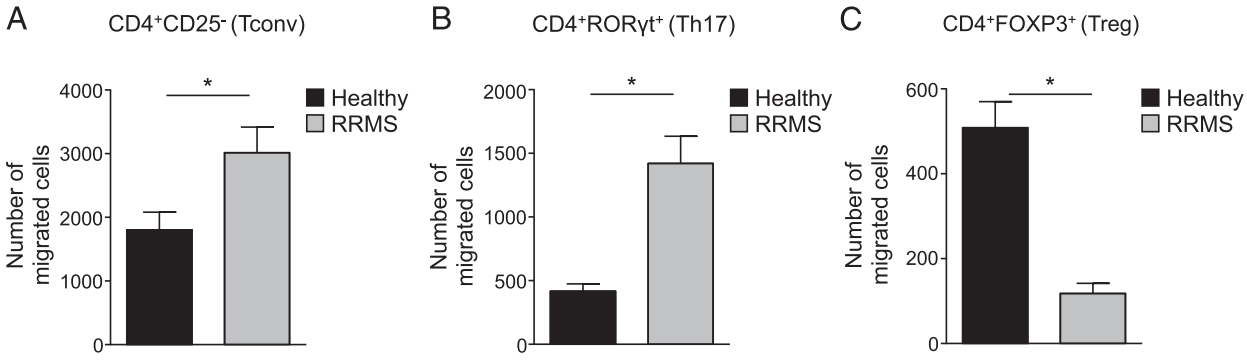

FIGURE 4. Altered migration of different freshly isolated T cell subsets from naive-to-treatment RRMS subjects as compared with healthy subjects in an in vitro BBB model. Freshly isolated PBMCs from healthy or naive-to-treatment RRMS subjects were put in contact with hCMEC/D3 brain microvascular endothelial cells on transwell polycarbonate filters. After 4 h coculture, number of migrated (**A**) $CD4^+CD25^-$ (Tconv) cells from healthy (n = 12) and naive-to-treatment RRMS (n = 12) subjects, (**B**) $CD4^+$ $ROR\gamma t^+$ (Th17) cells from healthy (n = 5) and naive-to-treatment RRMS (n = 4) subjects, and (**C**) $CD4^+FOXP3^+$ (Treg) cells from healthy (n = 5) and naive-to-treatment RRMS (n = 10) subjects were evaluated by FACS analysis; data are from 12 ($CD4^+CD25^-$ [Tconv]), five ($CD4^+$ $ROR\gamma t^+$ [Th17] cells), or 10 ($CD4^+FOXP3^+$ (Treg) cells) independent experiments. Statistical analysis was performed by using Mann–Whitney U test (two tails) (mean ± SEM). $*p \leq 0.05$.

proliferation of purified Tconv and Treg cells, isolated from healthy and RRMS subjects and stimulated with anti-CD3/CD28–coated beads for 60–72 h in culture medium supplemented with 5% AS. As shown in Fig. 5D, 5E, ANXA1 did not affect the proliferation of TCR-stimulated Tconv and Treg cells, both in healthy and RRMS individuals. We also observed that ANXA1 did not affect Treg cell function, evaluated as their ability to suppress Tconv cell proliferation in coculture experiments, both in healthy and RRMS individuals (Fig. 5F). These results suggest that ANXA1 reduced T cell activation in healthy individuals, but this phenomenon was impaired in subjects with RRMS.

ANXA1 impairs T cell priming via STAT3-dependent inhibition of monocyte maturation

Because the inhibitory effect of ANXA1 was observed only in the presence of a mixed leukocyte population, this led us to hypothesize a direct action on APCs rather than on T cells. For this reason, we evaluated the expression of several activation markers involved in T cell priming and activation in PBLs, in monocytes and B cells, representing the main APCs present in the mixed TCR-stimulated PBMCs culture. We found that ANXA1 treatment reduced the expression of ICAM-1, MHC class II (MHC II), CD80, CD86, and CD83 in PBLs of healthy subjects, but not in RRMS subjects (Fig. 6A, 6B), likely explaining why we did not observe a significant reduction of T cell proliferation in these subjects (Fig. 5A). The same analysis was performed on B cells, but we did not observe any difference upon ANXA1 treatment in this cellular subset (Supplemental Fig. 4E). Further analysis on monocytes (gated on $CD14^+$) also confirmed that ANXA1 profoundly reduced the expression of CD80, CD86, and CD83 on monocytes of healthy subjects, but not of RRMS subjects (Fig. 6C, 6D). Biochemical analysis performed on monocytes isolated from healthy subjects and stimulated in vitro with LPS (1 h) revealed an hyperactivation of the STAT3 pathway after an acute pretreatment (1 h) with ANXA1 (Fig. 6E). This suggests that ANXA1 could exert its anti-inflammatory role through a direct effect on STAT3 pathway, already known to impair the expression of costimulatory molecules on APCs with resulting decrease in T cell priming (40, 41). In this context, it has also recently been shown that IL-6 reduces the expression of MHC II and CD86 in human dendritic cells induced from PBMCs of healthy donors via STAT3 activation (42, 43). To this aim, we measured IL-6 production in culture supernatants and found an increased IL-6 secretion after ANXA1 treatment in TCR-stimulated PBMCs from healthy subjects (Fig. 6F); this, together with a direct ANXA1-dependent STAT3 activation, could contribute to sustain the STAT3 hyperactivation, leading to the impairment of monocyte maturation upon ANXA1 treatment. Moreover, we measured ANXA1 receptor, FPR2, to exclude that its reduced expression could account for the differential effect that ANXA1 exerted in healthy versus RRMS subjects. We analyzed PBMCs, $CD14^+$, $CD4^+$, and $CD4^+CD25^+$ isolated from healthy ad RRMS subjects and found a slight increase of FPR2 expression in RRMS, reaching the statistical significance only in the PBMCs population (Supplemental Fig. 4F–I). All our data reveal that, through a direct control of monocyte maturation, ANXA1 has a key role in the regulation of T lymphocyte activation in human healthy subjects, but this process is impaired during MS.

Discussion

Pathophysiological mechanisms contributing to the development of MS have been intensively investigated, with a major focus on the role of immune system in the inflammatory process. An imbalance between pro- and anti-inflammatory actions is believed to be important in the development and progression of MS (44).

ANXA1, a glucocorticoid-inducible protein abundantly expressed in neutrophils and innate immune cells, has long been known as a potent anti-inflammatory mediator (11, 45). Several studies suggest that its mechanism of action is mainly related to a direct action on monocytes, involving both transcriptional changes as well as rapid posttranslational effects (28, 29, 46). Glucocorticoids directly attenuate leukocyte extravasation by inhibiting endothelial transcription of E-selectin and VCAM (VCAM-1) but also dampen TCR signaling, resulting in reduced proliferative responses and cytokine production, including reduced IL-2 secretion (47–49). A series of reports have also shown that glucocorticoids induce de novo synthesis as well as translocation of ANXA1 to the cell surface in PBMCs (50, 51). ANXA1 can act dually either as an endogenous signaling molecule or as a secreted mediator (52). The expression of this molecule and its release in the extracellular milieu may thus serve as an indicator of the endogenous anti-inflammatory state. However, only few and controversial studies have investigated whether ANXA1 impacts on human T cell function (17–22).

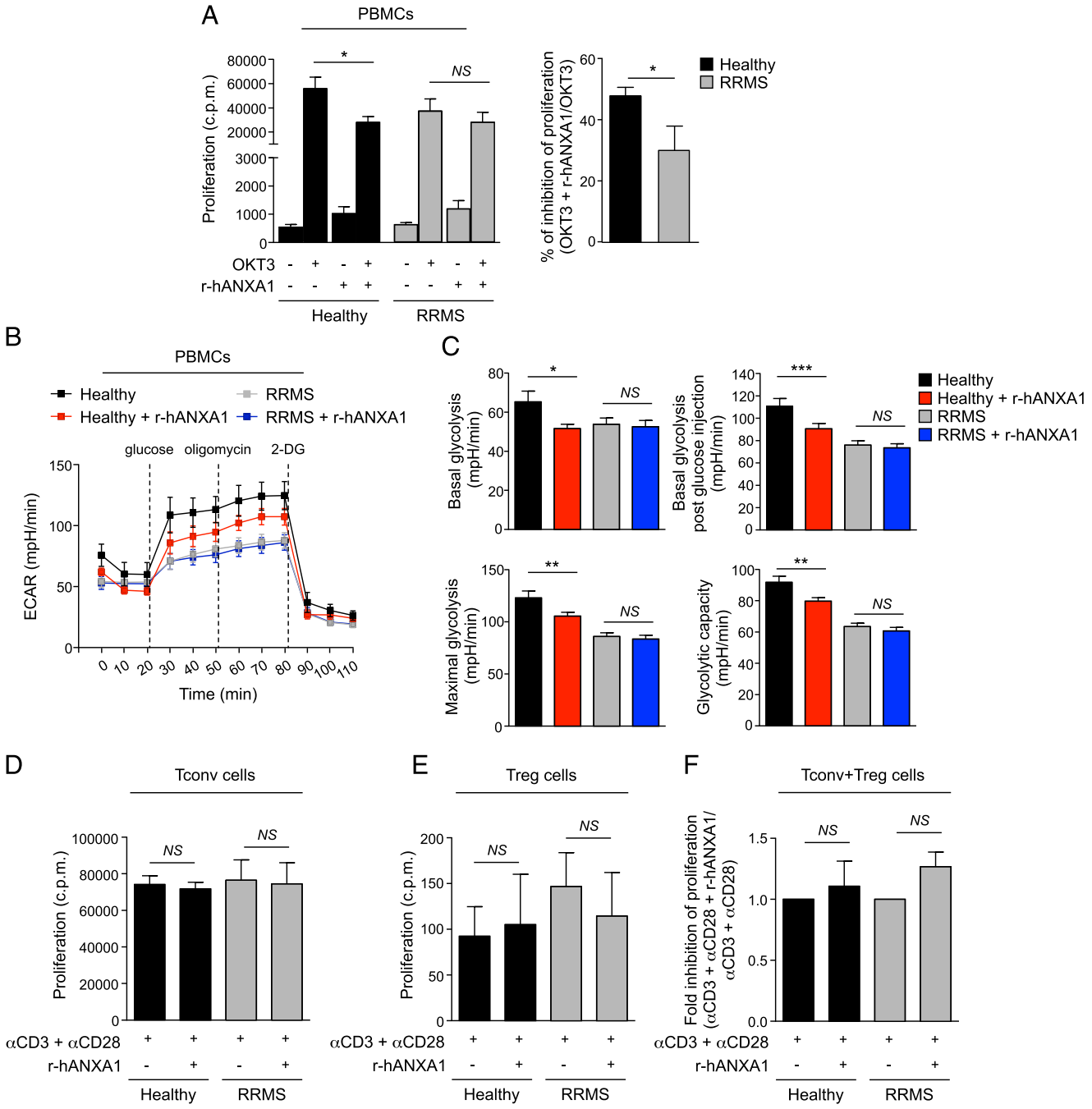

FIGURE 5. r-hANXA1 treatment affects engagement of glycolysis and proliferation of in vitro TCR–stimulated PBMCs from healthy, but not naive-to-treatment RRMS, subjects. (**A**) Proliferation (left) and percentage of inhibition of proliferation (right) of PBMCs from healthy (n = 7) and naive-to-treatment RRMS (n = 5) subjects, stimulated with OKT3 in the presence or in the absence of r-hANXA1 for 60–72 h; data are from seven independent experiments; comparisons within and between healthy and naive-to-treatment RRMS subjects are evaluated using paired Wilcoxon test (two tails) and Mann–Whitney U test (two tails), respectively (mean ± SEM). *$p \leq 0.01$. (**B**) Kinetic profile of ECAR as indicator of glycolysis in PBMCs from healthy (n = 3) and naive-to-treatment RRMS (n = 5) subjects, stimulated with OKT3 for 12 h, in the presence or in the absence of r-hANXA1. Dotted lines indicate the injections of compounds: glucose, the ATP-synthase inhibitor oligomycin and 2DG. Data report mean ± SEM of three measurements and are representative of six independent experiments in duplicates or triplicates. (**C**) Glycolytic parameters are calculated from ECAR profile: basal glycolysis, basal glycolysis after glucose injection, maximal glycolysis, and glycolytic capacity. Statistical analysis was performed by paired Wilcoxon test (two tails) (mean ± SEM). *$p \leq 0.05$, **$p \leq 0.001$, ***$p \leq 0.0001$. Proliferation of (**D**) Tconv and (**E**) Treg cells from healthy (n = 3) and naive-to-treatment RRMS (n = 3) subjects stimulated with anti-CD3 + anti-CD28 (αCD3 + αCD28) mAbs in the presence or in the absence of r-hANXA1 for 60–72 h. (**F**) Fold inhibition of proliferation of Tconv cocultured with Treg cells at a ratio of 1:1 in the presence or in the absence of r-hANXA1, presented relative to results obtained for Tconv cells stimulated with anti-CD3 + anti-CD28 mAbs from healthy (n = 3) and naive-to-treatment RRMS (n = 3) subjects. Data are from three independent experiments. Statistical analysis was performed by paired Wilcoxon test (two tails) (mean ± SEM).

In this study, we measured circulating ANXA1 levels in a large cohort of naive-to-treatment RRMS subjects and related it to their clinical status. Among all clinical parameters evaluated (gadolinium-enhancing lesions, spinal cord lesions, number of relapses prediagnosis, and EDSS), we found that ANXA1 levels inversely correlated with EDSS and number of relapses (both

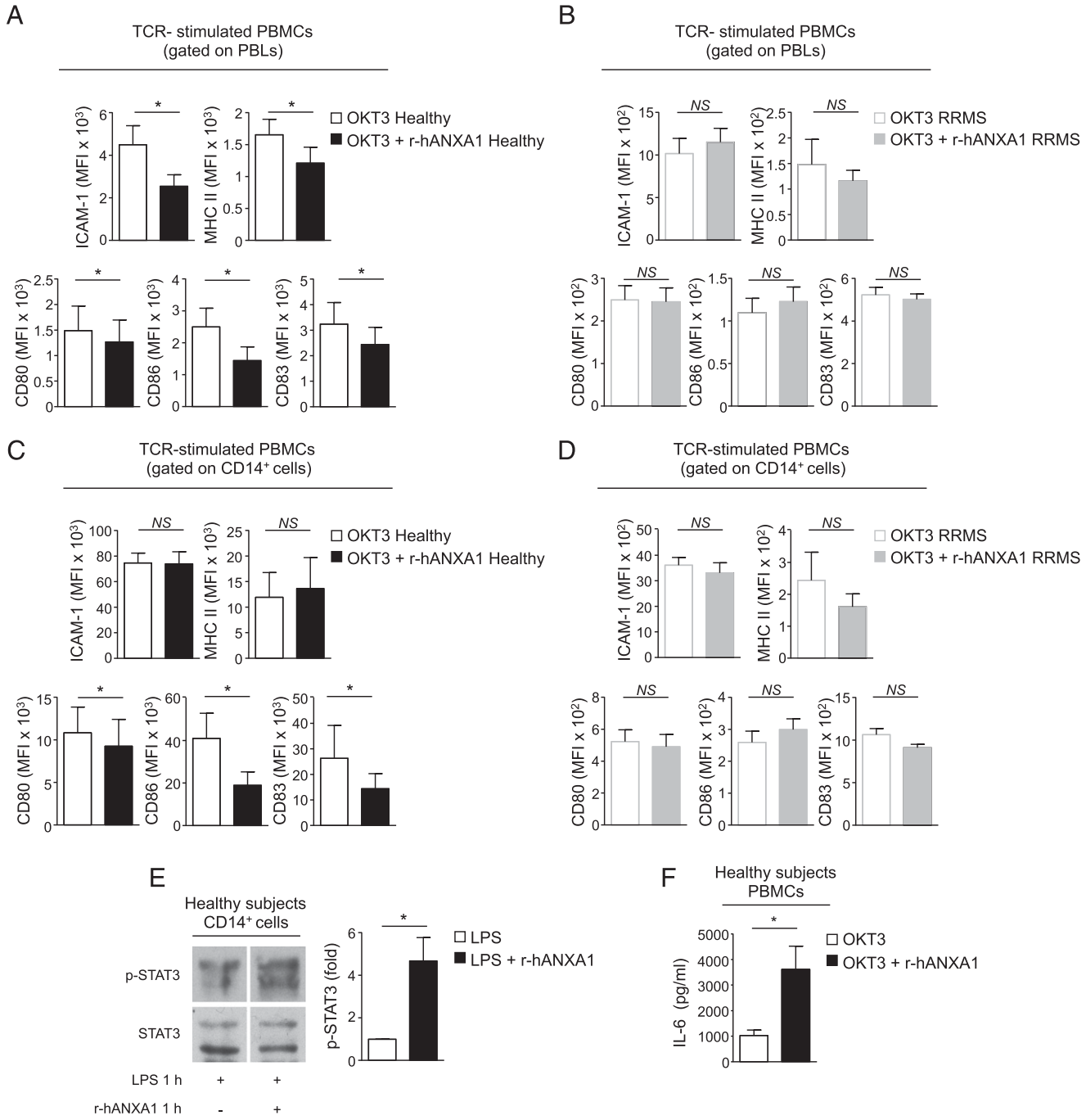

FIGURE 6. r-hANXA1 reduces the expression of different activation markers on TCR-stimulated lymphocytes and monocytes from healthy subjects, but not in naive-to-treatment RRMS subjects, via STAT3 signaling pathway. Mean fluorescence intensity (MFI) (referred to the whole population) of ICAM-1, MHC II, CD80, CD86, and CD83 expression on (**A** and **B**) PBLs and (**C** and **D**) monocytes (gated as $CD14^+$) in PBMCs of healthy ($n = 6$) and naive-to-treatment RRMS ($n = 4$) subjects stimulated for 36 h with OKT3 in the presence or in the absence of r-hANXA1. Data are from four (RRMS subjects) or six (healthy subjects) independent experiments; statistical analysis was performed by using paired Wilcoxon test (two tails) (mean ± SEM). $*p \leq 0.05$. (**E**) Western blot analysis of STAT3 pathway in monocytes isolated from healthy subjects, pretreated or not with r-hANXA1 (1 h), and then stimulated with LPS (1 h). Right, densitometry of p-STAT3 normalized to total STAT3 presented relative to results obtained for monocytes treated with LPS alone. Data are from three independent experiments; statistical analysis was performed by using Wilcoxon test (two tails) (mean ± SEM). $*p \leq 0.05$. (**F**) IL-6 levels (picogram per milliliter) in culture supernatants from 24-h, OKT3-stimulated PBMCs of healthy subjects ($n = 7$), treated or not with r-hANXA1. Data are from seven independent experiments; statistical analysis was performed by using Wilcoxon test (two tails) (mean ± SEM). $*p \leq 0.05$.

parameters reflecting disease severity and clinical score) in our RRMS cohort of patients at diagnosis, before disease-modifying treatments. Because EDSS is critical in defining the clinical status of patients, as it includes multiple parameters of neural impairment that correlate with tissue and cell damage; this suggests a protective role in MS. We acknowledge, nonetheless, the limitation that EDSS does not identify mechanistically the individual contributing factors responsible for the overall assessment.

ANXA1 is expressed in human and mouse T cells but to a lower extent than in innate immune cells, such as neutrophils and monocytes (53, 54). We found that ANXA1 expression in different human T cell subsets, namely $CD4^+CD25^+$, $CD4^+CD25^-$ (Tconv), $CD4^+FOXP3^+$ (Treg), and $CD4^+ROR\gamma t^+$ (Th17), was significantly

lower in RRMS subjects as compared with healthy controls, both as total content and cell surface level. Because ANXA1 is an endogenous anti-inflammatory mediator (and to ascertain that the differences we observed in freshly isolated T cells were not due to an increased recruitment/localization of $ANXA1^+$ T cells into the CNS), we measured its expression levels in TCR-stimulated T cells. Compared with healthy controls, RRMS subjects exhibited a significant reduction in ANXA1 production (both as total content and cell surface expression) in Treg cells, Th17 cells, and $CD25^{High}$ T cells. This, together with data obtained in freshly isolated T cells, confirmed a strong impairment of T cell–derived ANXA1 production during MS.

A key anti-inflammatory property of ANXA1 is its ability to inhibit leukocyte transmigration via a modulation of adhesion, molecule-based, leukocyte-endothelium interactions (12). Activated leukocytes (mainly neutrophils) mobilize their endogenous ANXA1 to the plasma membrane that is then secreted to promote leukocyte detachment from endothelial cells, thus functioning as a negative regulator of the transmigratory process (55, 56). Several studies reported that ANXA1 binds α4β1 integrin on leukocytes to prevent its interaction with VCAM-1 and/or to cause L-selectin shedding from leukocytes in a calcium-dependent manner, preventing the tethering, rolling, and firm adhesion of leukocytes to the endothelium necessary for transmigration (12, 57). Because T cell migration into the CNS is a crucial event for Ag-specific T cell activation in MS (58), we asked whether a reduced expression of ANXA1 could be associated with an increased T cell migration in RRMS subjects. We used an in vitro BBB model represented by human hCMEC/D3 cells polarized on transwell to allow correct tightness (25). Downmodulation of ANXA1 expression in Th17 cells corresponded to a higher degree of migration, likely contributing to facilitate the proinflammatory activity of these cells. On the contrary, downmodulation of ANXA1 in anti-inflammatory Treg cells was not beneficial to migration and capacity to control tissue damage. Being ANXA1, an endogenous molecule involved in the resolution of inflammation (10, 17, 18), these different effects could reflect divergent mechanisms of action of ANXA1 on proinflammatory Th17 and Treg cells. Both the reduced expression of ANXA1 on proinflammatory T cell subsets, together with the loss of ANXA1 in the brain microvascular endothelium previously described in MS subjects (23), could contribute to higher degree of leukocyte infiltration into the CNS.

Although the anti-inflammatory activity of exogenous ANXA1 has been established in different in vivo and in vitro models (19, 23, 34), a global analysis of effects in human T cell subsets have never been assessed. Several investigators demonstrated that ANXA1 exerts an inhibitory effect on adaptive immune response in vivo (59, 60) and during Ag-specific T cell activation in vitro (20, 33). Other studies revealed that ANXA1 promotes Th1 while inhibiting Th2 responses (21). In this study, we evaluated the impact of ANXA1 on human PBMCs, Tconv and Treg cells isolated from healthy or RRMS subjects and in vitro activated through the TCR. We found that ANXA1 impaired engagement of glycolysis and proliferation of in vitro TCR–stimulated PBMCs from healthy, but not naive-to-treatment RRMS, subjects. However, this different behavior in RRMS subjects was not secondary to a reduced expression of ANXA1 receptor (FPR2) on target cells, but to a different effect, ANXA1 exerted on TCR-related signaling and AKT pathway, as testified by reduced TCR/ZAP-70 activity and AKT phosphorylation observed in PBMCs of healthy, but not RRMS, subjects. Strikingly, ANXA1 neither affected the proliferation of TCR-stimulated Tconv and Treg cells nor Treg cell suppressive ability, both in healthy and naive-to-treatment RRMS subjects. Our data revealed that when ANXA1 was added to TCR-engaged PBMCs, there was an impairment of T cell activation and a reduction in the expression of several activation markers (ICAM-1, MHC II, CD80, CD86, and CD83), secondarily to an inhibitory effect on human monocytes, which are major APCs in PBMCs. It affected maturation of monocytes from human healthy subjects, as testified by a reduced expression of several costimulatory molecules, such as CD80, CD86, and CD83 (61, 62). This means that the reduced T cell proliferation observed is secondary to an altered T cell priming, and not to a direct effect on T cells. Interestingly, ANXA1 did not affect the expression of costimulatory molecules on monocytes of RRMS subjects, likely explaining why we did not detect a significant impairment of T cell activation in our cohort.

Treatment of monocytes from human healthy subjects with ANXA1 affected LPS-induced in vitro maturation. This phenomenon was secondary to a hyperactivation of the STAT3 pathway, known to exert an inhibitory effect during monocyte maturation (40, 41).

Our data highlight the significance of ANXA1 as part of the endogenous immunosuppressive circuit and couple its anti-inflammatory action to STAT3 signaling pathway. This ANXA1-dependent STAT3 hyperactivation is also supported by an increased IL-6 production in TCR-stimulated PBMCs cultured in the presence of ANXA1. Several reports indeed suggest that the IL-6/STAT3 pathway leads to the suppression of TLR4 ligand and LPS-induced APC maturation and activation (42, 43). Also, it has been shown that STAT3 hyperactivation suppresses CD86 and MHC II expression on human APCs, thus limiting Ag-specific $CD4^+$ T cell activation (41, 63). Our results are in agreement with other reports showing that ANXA1 was able to elicit rapid anti-inflammatory effects by inhibiting neutrophil extravasation and activating a specific gene program that leads to the induction of an anti-inflammatory phenotype (56, 64). Indeed, ANXA1 is an endogenous determinant of proresolving properties of cAMP-elevating agents and cAMP-mimetic drugs (65). Also, thanks to its ability to bind α4β1 integrin (very late Ag 4, VLA4) on the cell surface, ANXA1 acts as an endogenous inhibitor of the leukocyte recruitment into the CNS (12, 36). This pathway is specifically targeted by a very effective second line drug for MS, the mAb natalizumab (66). Therefore, proresolving ANXA1-based therapies could control inflammation using the pathway shared with natalizumab.

Taken together, our results help to elucidate the role of ANXA1 on human T cells, both in healthy conditions and during MS, and pinpoint the key anti-inflammatory mediator ANXA1 as part of the counter-regulatory circuits elicited by interfering with the process of human monocyte activation and leukocyte recruitment.

By unveiling a systemic reduction of ANXA1, particularly evident in RRMS subjects with higher disability, our findings indicate that loss of ANXA1-mediated anti-inflammatory function could represent a novel mechanism of immune dysfunction in the pathogenesis of MS.

Acknowledgments

We apologize to colleagues whose work could not be cited in this study because of space limitations. We thank M. Montagna and S. De Simone for technical support, K. Schmierer (Blizard Institute, Barts and The London School of Medicine and Dentistry, Queen Mary University of London, London, U.K., and Clinical Board Medicine, The Royal London Hospital, Barts Health National Health Service Trust, London, U.K.) for supplying patients' blood samples used in the studies of PBMC migration, and Ornella Moreggia (Dipartimento di Neurologia, Centro Regionale Sclerosi Multipla, Azienda Ospedaliera "A. Cardarelli,"

Naples, Italy) for the collection of clinical information of RRMS subjects.

Disclosures

The authors have no financial conflicts of interest.

References

1. Luster, A. D., R. Alon, and U. H. von Andrian. 2005. Immune cell migration in inflammation: present and future therapeutic targets. *Nat. Immunol.* 6: 1182–1190.
2. Ward, P. A., and A. B. Lentsch. 1999. The acute inflammatory response and its regulation. *Arch. Surg.* 134: 666–669.
3. Nylander, A., and D. A. Hafler. 2012. Multiple sclerosis. *J. Clin. Invest.* 122: 1180–1188.
4. Gilgun-Sherki, Y., E. Melamed, and D. Offen. 2004. The role of oxidative stress in the pathogenesis of multiple sclerosis: the need for effective antioxidant therapy. *J. Neurol.* 251: 261–268.
5. Hedegaard, C. J., M. Krakauer, K. Bendtzen, H. Lund, F. Sellebjerg, and C. H. Nielsen. 2008. T helper cell type 1 (Th1), Th2 and Th17 responses to myelin basic protein and disease activity in multiple sclerosis. *Immunology* 125: 161–169.
6. Gayo, A., L. Mozo, A. Suárez, A. Tuñon, C. Lahoz, and C. Gutiérrez. 1998. Glucocorticoids increase IL-10 expression in multiple sclerosis patients with acute relapse. *J. Neuroimmunol.* 85: 122–130.
7. Lindquist, S., S. Hassinger, J. A. Lindquist, and M. Sailer. 2011. The balance of pro-inflammatory and trophic factors in multiple sclerosis patients: effects of acute relapse and immunomodulatory treatment. *Mult. Scler.* 17: 851–866.
8. Xu, L., Z. Xu, and M. Xu. 2009. Glucocorticoid treatment restores the impaired suppressive function of regulatory T cells in patients with relapsing-remitting multiple sclerosis. *Clin. Exp. Immunol.* 158: 26–30.
9. Frequin, S. T., F. Barkhof, K. J. Lamers, and O. R. Hommes. 1992. The effects of high-dose methylprednisolone on gadolinium-enhanced magnetic resonance imaging and cerebrospinal fluid measurements in multiple sclerosis. *J. Neuroimmunol.* 40: 265–272.
10. Perretti, M., and F. D'Acquisto. 2009. Annexin A1 and glucocorticoids as effectors of the resolution of inflammation. *Nat. Rev. Immunol.* 9: 62–70.
11. McArthur, S., E. Cristante, M. Paterno, H. Christian, F. Roncaroli, G. E. Gillies, and E. Solito. 2010. Annexin A1: a central player in the anti-inflammatory and neuroprotective role of microglia. *J. Immunol.* 185: 6317–6328.
12. Solito, E., I. A. Romero, S. Marullo, F. Russo-Marie, and B. B. Weksler. 2000. Annexin 1 binds to U937 monocytic cells and inhibits their adhesion to microvascular endothelium: involvement of the alpha 4 beta 1 integrin. *J. Immunol.* 165: 1573–1581.
13. Spurr, L., S. Nadkarni, M. Pederzoli-Ribeil, N. J. Goulding, M. Perretti, and F. D'Acquisto. 2011. Comparative analysis of Annexin A1-formyl peptide receptor 2/ALX expression in human leukocyte subsets. *Int. Immunopharmacol.* 11: 55–66.
14. Kim, S. W., H. J. Rhee, J. Ko, Y. J. Kim, H. G. Kim, J. M. Yang, E. C. Choi, and D. S. Na. 2001. Inhibition of cytosolic phospholipase A2 by annexin I. Specific interaction model and mapping of the interaction site. *J. Biol. Chem.* 276: 15712–15719.
15. Ayroldi, E., L. Cannarile, G. Migliorati, G. Nocentini, D. V. Delfino, and C. Riccardi. 2012. Mechanisms of the anti-inflammatory effects of glucocorticoids: genomic and nongenomic interference with MAPK signaling pathways. *FASEB J.* 26: 4805–4820.
16. Ramdas, J., and J. M. Harmon. 1998. Glucocorticoid-induced apoptosis and regulation of NF-kappaB activity in human leukemic T cells. *Endocrinology* 139: 3813–3821.
17. Sheikh, M. H., and E. Solito. 2018. Annexin A1: uncovering the many talents of an old protein. *Int. J. Mol. Sci.* 19: E1045.
18. Yang, Y. H., E. F. Morand, S. J. Getting, M. Paul-Clark, D. L. Liu, S. Yona, R. Hannon, J. C. Buckingham, M. Perretti, and R. J. Flower. 2004. Modulation of inflammation and response to dexamethasone by Annexin 1 in antigen-induced arthritis. *Arthritis Rheum.* 50: 976–984.
19. Ng, F. S., K. Y. Wong, S. P. Guan, F. B. Mustafa, T. S. Kajiji, P. Bist, S. K. Biswas, W. S. Wong, and L. H. Lim. 2011. Annexin-1-deficient mice exhibit spontaneous airway hyperresponsiveness and exacerbated allergen-specific antibody responses in a mouse model of asthma. *Clin. Exp. Allergy* 41: 1793–1803.
20. D'Acquisto, F., A. Merghani, E. Lecona, G. Rosignoli, K. Raza, C. D. Buckley, R. J. Flower, and M. Perretti. 2007. Annexin-1 modulates T-cell activation and differentiation. *Blood* 109: 1095–1102.
21. D'Acquisto, F., N. Paschalidis, A. L. Sampaio, A. Merghani, R. J. Flower, and M. Perretti. 2007. Impaired T cell activation and increased Th2 lineage commitment in Annexin-1-deficient T cells. *Eur. J. Immunol.* 37: 3131–3142.
22. Paschalidis, N., A. J. Iqbal, F. Maione, E. G. Wood, M. Perretti, R. J. Flower, and F. D'Acquisto. 2009. Modulation of experimental autoimmune encephalomyelitis by endogenous annexin A1. *J. Neuroinflammation* 6: 33.
23. Cristante, E., S. McArthur, C. Mauro, E. Maggioli, I. A. Romero, M. Wylezinska-Arridge, P. O. Couraud, J. Lopez-Tremoleda, H. C. Christian, B. B. Weksler, et al. 2013. Identification of an essential endogenous regulator of blood-brain barrier integrity, and its pathological and therapeutic implications. *Proc. Natl. Acad. Sci. USA* 110: 832–841.
24. Polman, C. H., S. C. Reingold, B. Banwell, M. Clanet, J. A. Cohen, M. Filippi, K. Fujihara, E. Havrdova, M. Hutchinson, L. Kappos, et al. 2011. Diagnostic criteria for multiple sclerosis: 2010 revisions to the McDonald criteria. *Ann. Neurol.* 69: 292–302.
25. Weksler, B., I. A. Romero, and P. O. Couraud. 2013. The hCMEC/D3 cell line as a model of the human blood brain barrier. *Fluids Barriers CNS* 10: 16.
26. De Rosa, V., C. Procaccini, G. Calì, G. Pirozzi, S. Fontana, S. Zappacosta, A. La Cava, and G. Matarese. 2007. A key role of leptin in the control of regulatory T cell proliferation. *Immunity* 26: 241–255.
27. Solito, E., A. Kamal, F. Russo-Marie, J. C. Buckingham, S. Marullo, and M. Perretti. 2003. A novel calcium-dependent proapoptotic effect of annexin 1 on human neutrophils. *FASEB J.* 17: 1544–1546.
28. Perretti, M., F. Ingegnoli, S. K. Wheller, M. C. Blades, E. Solito, and C. Pitzalis. 2002. Annexin 1 modulates monocyte-endothelial cell interaction in vitro and cell migration in vivo in the human SCID mouse transplantation model. *J. Immunol.* 169: 2085–2092.
29. Solito, E., H. C. Christian, M. Festa, A. Mulla, T. Tierney, R. J. Flower, and J. C. Buckingham. 2006. Post-translational modification plays an essential role in the translocation of annexin A1 from the cytoplasm to the cell surface. *FASEB J.* 20: 1498–1500.
30. Kumar, M., N. Putzki, V. Limmroth, R. Remus, M. Lindemann, D. Knop, N. Mueller, C. Hardt, E. Kreuzfelder, and H. Grosse-Wilde. 2006. CD4+CD25+FoxP3+ T lymphocytes fail to suppress myelin basic protein-induced proliferation in patients with multiple sclerosis. *J. Neuroimmunol.* 180: 178–184.
31. Kebir, H., K. Kreymborg, I. Ifergan, A. Dodelet-Devillers, R. Cayrol, M. Bernard, F. Giuliani, N. Arbour, B. Becher, and A. Prat. 2007. Human TH17 lymphocytes promote blood-brain barrier disruption and central nervous system inflammation. *Nat. Med.* 13: 1173–1175.
32. Hannon, R., J. D. Croxtall, S. J. Getting, F. Roviezzo, S. Yona, M. J. Paul-Clark, F. N. Gavins, M. Perretti, J. F. Morris, J. C. Buckingham, and R. J. Flower. 2003. Aberrant inflammation and resistance to glucocorticoids in annexin $1^{-/-}$ mouse. *FASEB J.* 17: 253–255.
33. Kamal, A. M., S. F. Smith, M. De Silva Wijayasinghe, E. Solito, and C. J. Corrigan. 2001. An annexin 1 (ANXA1)-derived peptide inhibits prototype antigen-driven human T cell Th1 and Th2 responses in vitro. *Clin. Exp. Allergy* 31: 1116–1125.
34. Girol, A. P., K. K. Mimura, C. C. Drewes, S. M. Bolonheis, E. Solito, S. H. Farsky, C. D. Gil, and S. M. Oliani. 2013. Anti-inflammatory mechanisms of the annexin A1 protein and its mimetic peptide Ac2-26 in models of ocular inflammation in vivo and in vitro. *J. Immunol.* 190: 5689–5701.
35. Miskov-Zivanov, N., M. S. Turner, L. P. Kane, P. A. Morel, and J. R. Faeder. 2013. The duration of T cell stimulation is a critical determinant of cell fate and plasticity. *Sci. Signal.* 6: ra97.
36. McArthur, S., R. A. Loiola, E. Maggioli, M. Errede, D. Virgintino, and E. Solito. 2016. The restorative role of annexin A1 at the blood-brain barrier. *Fluids Barriers CNS* 13: 17.
37. Sonar, S. A., and G. Lal. 2017. Differentiation and transmigration of CD4 T cells in neuroinflammation and autoimmunity. *Front. Immunol.* 8: 1695.
38. Pearce, E. L., and E. J. Pearce. 2013. Metabolic pathways in immune cell activation and quiescence. *Immunity* 38: 633–643.
39. De Rosa, V., M. Galgani, A. Porcellini, A. Colamatteo, M. Santopaolo, C. Zuchegna, A. Romano, S. De Simone, C. Procaccini, C. La Rocca, et al. 2015. Glycolysis controls the induction of human regulatory T cells by modulating the expression of FOXP3 exon 2 splicing variants. *Nat. Immunol.* 16: 1174–1184.
40. Pupjalis, D., J. Goetsch, D. J. Kottas, V. Gerke, and U. Rescher. 2011. Annexin A1 released from apoptotic cells acts through formyl peptide receptors to dampen inflammatory monocyte activation via JAK/STAT/SOCS signalling. *EMBO Mol. Med.* 3: 102–114.
41. Cheng, F., H. W. Wang, A. Cuenca, M. Huang, T. Ghansah, J. Brayer, W. G. Kerr, K. Takeda, S. Akira, S. P. Schoenberger, et al. 2003. A critical role for Stat3 signaling in immune tolerance. *Immunity* 19: 425–436.
42. Park, S. J., T. Nakagawa, H. Kitamura, T. Atsumi, H. Kamon, S. Sawa, D. Kamimura, N. Ueda, Y. Iwakura, K. Ishihara, et al. 2004. IL-6 regulates in vivo dendritic cell differentiation through STAT3 activation. *J. Immunol.* 173: 3844–3854.
43. Ohno, Y., H. Kitamura, N. Takahashi, J. Ohtake, S. Kaneumi, K. Sumida, S. Homma, H. Kawamura, N. Minagawa, S. Shibasaki, and A. Taketomi. 2016. IL-6 down-regulates HLA class II expression and IL-12 production of human dendritic cells to impair activation of antigen-specific CD4(+) T cells. *Cancer Immunol. Immunother.* 65: 193–204.
44. Wu, G. F., and E. Alvarez. 2011. The immunopathophysiology of multiple sclerosis. *Neurol. Clin.* 29: 257–278.
45. Perretti, M., J. D. Croxtall, S. K. Wheller, N. J. Goulding, R. Hannon, and R. J. Flower. 1996. Mobilizing lipocortin 1 in adherent human leukocytes downregulates their transmigration. *Nat. Med.* 2: 1259–1262.
46. Lange, C., D. J. Starrett, J. Goetsch, V. Gerke, and U. Rescher. 2007. Transcriptional profiling of human monocytes reveals complex changes in the expression pattern of inflammation-related genes in response to the annexin A1-derived peptide Ac1-25. *J. Leukoc. Biol.* 82: 1592–1604.
47. Filep, J. G., A. Delalandre, Y. Payette, and E. Földes-Filep. 1997. Glucocorticoid receptor regulates expression of L-selectin and CD11/CD18 on human neutrophils. *Circulation* 96: 295–301.
48. Yusuf-Makagiansar, H., M. E. Anderson, T. V. Yakovleva, J. S. Murray, and T. J. Siahaan. 2002. Inhibition of LFA-1/ICAM-1 and VLA-4/VCAM-1 as a therapeutic approach to inflammation and autoimmune diseases. *Med. Res. Rev.* 22: 146–167.
49. Cain, D. W., and J. A. Cidlowski. 2017. Immune regulation by glucocorticoids. *Nat. Rev. Immunol.* 17: 233–247.

50. Goulding, N. J., J. L. Godolphin, P. R. Sharland, S. H. Peers, M. Sampson, P. J. Maddison, and R. J. Flower. 1990. Anti-inflammatory lipocortin 1 production by peripheral blood leucocytes in response to hydrocortisone. *Lancet* 335: 1416–1418.
51. Sudlow, A. W., F. Carey, R. Forder, and N. J. Rothwell. 1996. The role of lipocortin-1 in dexamethasone-induced suppression of PGE2 and TNF alpha release from human peripheral blood mononuclear cells. *Br. J. Pharmacol.* 117: 1449–1456.
52. Bena, S., V. Brancaleone, J. M. Wang, M. Perretti, and R. J. Flower. 2012. Annexin A1 interaction with the FPR2/ALX receptor: identification of distinct domains and downstream associated signaling. *J. Biol. Chem.* 287: 24690–24697.
53. Dalli, J., C. P. Jones, D. M. Cavalcanti, S. H. Farsky, M. Perretti, and S. M. Rankin. 2012. Annexin A1 regulates neutrophil clearance by macrophages in the mouse bone marrow. *FASEB J.* 26: 387–396.
54. Gavins, F. N., and M. J. Hickey. 2012. Annexin A1 and the regulation of innate and adaptive immunity. *Front. Immunol.* 3: 354.
55. Gavins, F. N., S. Yona, A. M. Kamal, R. J. Flower, and M. Perretti. 2003. Leukocyte antiadhesive actions of annexin 1: ALXR- and FPR-related anti-inflammatory mechanisms. *Blood* 101: 4140–4147.
56. Chatterjee, B. E., S. Yona, G. Rosignoli, R. E. Young, S. Nourshargh, R. J. Flower, and M. Perretti. 2005. Annexin 1-deficient neutrophils exhibit enhanced transmigration in vivo and increased responsiveness in vitro. *J. Leukoc. Biol.* 78: 639–646.
57. de Coupade, C., E. Solito, and J. D. Levine. 2003. Dexamethasone enhances interaction of endogenous annexin 1 with L-selectin and triggers shedding of L-selectin in the monocytic cell line U-937. *Br. J. Pharmacol.* 140: 133–145.
58. Engelhardt, B., and R. M. Ransohoff. 2005. The ins and outs of T-lymphocyte trafficking to the CNS: anatomical sites and molecular mechanisms. *Trends Immunol.* 26: 485–495.
59. D'Acquisto, F., M. Perretti, and R. J. Flower. 2008. Annexin-A1: a pivotal regulator of the innate and adaptive immune systems. *Br. J. Pharmacol.* 155: 152–169.
60. Yang, Y. H., W. Song, J. A. Deane, W. Kao, J. D. Ooi, D. Ngo, A. R. Kitching, E. F. Morand, and M. J. Hickey. 2013. Deficiency of annexin A1 in CD4+ T cells exacerbates T cell-dependent inflammation. *J. Immunol.* 190: 997–1007.
61. Huggins, A., N. Paschalidis, R. J. Flower, M. Perretti, and F. D'Acquisto. 2009. Annexin-1-deficient dendritic cells acquire a mature phenotype during differentiation. *FASEB J.* 23: 985–996.
62. Weyd, H., L. Abeler-Dörner, B. Linke, A. Mahr, V. Jahndel, S. Pfrang, M. Schnölzer, C. S. Falk, and P. H. Krammer. 2013. Annexin A1 on the surface of early apoptotic cells suppresses CD8+ T cell immunity. *PLoS One* 8: e62449.
63. Liu, W. H., J. J. Liu, J. Wu, L. L. Zhang, F. Liu, L. Yin, M. M. Zhang, and B. Yu, PLoS One Editors. 2018. Retraction: Novel mechanism of inhibition of dendritic cells maturation by mesenchymal stem cells via interleukin-10 and the JAK1/STAT3 signaling pathway. *PLoS One* 8: e0194455.
64. Sugimoto, M. A., J. P. Vago, M. M. Teixeira, and L. P. Sousa. 2016. Annexin A1 and the resolution of inflammation: modulation of neutrophil recruitment, apoptosis, and clearance. *J. Immunol. Res.* 2016: 8239258.
65. Lima, K. M., J. P. Vago, T. R. Caux, G. L. Negreiros-Lima, M. A. Sugimoto, L. P. Tavares, R. G. Arribada, A. A. F. Carmo, I. Galvão, B. R. C. Costa, et al. 2017. The resolution of acute inflammation induced by cyclic AMP is dependent on annexin A1. *J. Biol. Chem.* 292: 13758–13773.
66. Engelhardt, B., and L. Kappos. 2008. Natalizumab: targeting alpha4-integrins in multiple sclerosis. *Neurodegener. Dis.* 5: 16–22.